



Published in final edited form as:

Anal Chem. 2012 February 21; 84(4): 2067–2071. doi:10.1021/ac202934x.

Lifting gate PDMS microvalves and pumps for microfluidic control

Jungkyu Kim, Minjee Kang, Erik C. Jensen, and Richard A. Mathies*

Department of Chemistry, University of California, Berkeley, CA 94720

Abstract

We describe the development and characterization of pneumatically actuated “lifting gate” microvalves and pumps. A fluidic layer containing the gate structure and a pneumatic layer are fabricated by soft-lithography in PDMS and bonded permanently with an oxygen plasma treatment. The microvalve structures are then reversibly bonded to a featureless glass or plastic substrate to form hybrid glass-PDMS and plastic-PDMS microchannel structures. The breakthrough pressures of the microvalve increase linearly up to 65 kPa as the closing pressure increases. The pumping capability of these structures ranges from the nanoliter to microliter scale depending on the number of cycles and closing pressure employed. The micropump structures exhibit up to 86.2% pumping efficiency from flow rate measurements. The utility of these structures for integrated sample processing is demonstrated by performing an automated immunoassay. These lifting gate valve and pump structures enable facile integration of complex microfluidic control systems with a wide range of lab-on-a-chip substrates.

Keywords

microvalves; micropump; soft-lithography; microfluidics; automated immunoassay; lab-on-a-chip

Introduction

Microvalves and pumps are essential components for many microfluidic bioanalysis applications including genomic analysis,¹⁻⁴ pathogen detection,⁵⁻⁷ immunoassays,⁸⁻¹⁰ high-throughput cellular analysis¹¹⁻¹⁴ and automated sample processing.¹⁵ Mechanisms for microvalve actuation including electrical, thermal, chemical and pneumatic means have been developed and utilized for sample delivery and flow rate control.¹⁶ Pneumatically-actuated microvalves and pumps have been most widely employed for assay automation with large scale integration because this fabrication is simple and inexpensive.

The two most frequently used pneumatically-actuated microvalves and pumps were developed by the Quake group^{17, 18} and Mathies group¹⁹, respectively. Both use a flexible polydimethylsiloxane (PDMS) layer for actuation. In one case, overlapping multilayer soft lithography channel structures are used to form normally open microvalves in which a pressure applied to one channel expands into and pinches off the second channel. In contrast, normally closed monolithic membrane valves employ glass-PDMS-glass hybrid^{8, 19, 20} or PMMA-PDMS-PMMA structures with featureless membrane layers.²¹ This type of valve effectively closes against high pressures and enables precise control of nanoliter scale volumes. However, integration of these structures with downstream analyses

*Address correspondence to: Richard A. Mathies, Department of Chemistry, University of California, Berkeley, CA 94720, Phone: (510)642-4192, Fax:(510)642-3599, ramathies@berkeley.edu.

often requires the fabrication of via holes in the solid substrates for access between layers.²² The resulting increases in the dead volumes of the device and fabrication complexity are often problematic. Furthermore, patterning of surfaces within a microchannel with additional structures often requires intensive fabrication, and limits the reusability of the device.²³

Recently, a different normally-closed, pneumatically actuated microvalve design has been proposed by the Kenis group and utilized to control vacuum driven fluid flow.²⁴ This valve structure utilizes a flexible PDMS membrane with microfabricated barrier features (gates) that are lifted away from a substrate by vacuum to enable fluid flow. However, integrated fluid pumping and transport has not been demonstrated or characterized with this microvalve design.

In this paper, we demonstrate and characterize the integrated pumping capabilities of lifting gate microvalves (Figure 1A) and demonstrate the utility of these structures for facile integration with patterned, solid substrates. A pump is formed using a linear array of three microvalves in series with cyclic actuation. These unique structures enable direct integration with a broad range of substrates, thereby reducing microfabrication complexity. To demonstrate the utility of these microvalves and pumps, we perform an automated microparticle based immunoassay using a polyester terephthalate (PET) substrate. These microvalves and pumps are capable of highly efficient, automated fluidic transport and address several limitations of multilayer PDMS valves and monolithic membrane valves described above.

Materials and methods

Fabrication of lifting gate microvalves and pumps

A soft-lithography method using SU-8 molds was used to prepare channel features in PDMS layers. Figure 2 presents the steps employed for device fabrication and assembly. For fluidic and pneumatic layers, SU-8 molds were fabricated to obtain a 25 μm and 60 μm feature height, respectively. After silanizing the SU-8 molds using chemical vapor deposition (CVD), the mold for the fluidic layer was spin-coated with a 10 (base material): 1 (curing agent) ratio of PDMS (Dow Corning, USA) and thermally cured at 65 °C. PDMS thickness as a function of angular velocity was characterized to fabricate this system. (Figure S-1) In this study, the fluidic mold was spun with 350 rpm to fabricate the 200 μm thick PDMS membrane structure. For the pneumatic layer mold, PDMS was poured on the mold and cured on a 65 °C hotplate for one hour. Holes were punched in the PDMS replica for pneumatic connections and then it was permanently bonded to a PDMS channel layer using oxygen plasma activation (PETS Inc., USA). To evaluate the valving and pumping efficiency, the microvalves and pump structures were then bonded to the glass substrate by UV- ozone treatment.²⁵

Operation and characterization

Lifting gate microvalves and pumps were operated by applying a vacuum or pressure to inlets on the pneumatic layer (Figure 1B). The valves are actuated by a series of off-chip solenoid controllers using a vacuum pump (-87 kPa) and various closing pressures. Prior to operation of the devices, all microvalves were opened in the absence of fluid to reduce the bonding between glass and PDMS to increase the ease of actuation. To measure the breakthrough pressure of the micro valve, inlet and outlet valves were opened and the middle valve was held closed with various pressures (5~60 kPa). By varying the fluidic pressure on the inlet side, we determined the critical pressure required to initiate flow through the 2.25 mm diameter valve. To evaluate the pumping capability, five different sized pumps were

used to characterize the dependence of displacement chamber volume on pump performance. As described previously, the volume pumped per cycle depends on the volume of the center valve (manifold valve) in a three valve pump. The theoretical maximum volume pumped per cycle (V_{\max}) also depends to a lesser extent on the volume of the fluidic region on the downstream side of the gate since the PDMS can be deflected into this region. Taking this into account, V_{\max} was calculated as:

$$V_{\max} = \frac{1}{4} \pi D_{\text{chamber}}^2 d_{\text{manifold}} + A_i d_{\text{fluidic}}$$

where d_{manifold} , D_{chamber} , d_{fluidic} and A_i are the depth of the manifold valve displacement chamber, diameter of the manifold valve displacement chamber, depth of fluidic channel, and a half area of fluidic chamber, respectively (Figure 1 and Table S-1). Each of the input and output valves has an identical diameter ($D_{\text{chamber}} = 750 \mu\text{m}$). Standard 5-step pumping programs¹⁹ were used and volumetric flow rates were adjusted by changing the actuation time and closing pressure during the pumping programs.

Automated microparticle label immunoassay

To demonstrate the utility of the lifting-gate microvalves for integration and reusability with plastic substrates, a device was designed and fabricated as described above. In the first step of the assay, 100 $\mu\text{g}/\text{mL}$ of streptavidin (Sigma Aldrich, USA) was non-specifically adsorbed onto the polyester terephthalate (PET) film (Rogers Corp., IL, USA) for 2 hours in a 37 °C oven prior to assembly of the device. After UV ozone treatment of the PDMS layer, it was attached to the streptavidin treated polyester terephthalate (PET) substrate. One percent bovine serum albumin (BSA), biotinylated capture antibodies (Anti-mouse IgG-Fc specific from Thermo-Fisher Scientific Inc., USA), target sample (Mouse IgG, Thermo-Fisher Scientific Inc., USA), anti-mouse IgG conjugated microparticles (Abcam Inc. and MyOne Invitrogen Inc., USA) and washing buffer were selected via bus valves and pumped to the reactor to perform the immunoassay. To remove the unbound beads, hydrodynamic washing was performed for 2 minutes with a flow rate of 2.2 $\mu\text{L}/\text{min}$. After collecting the images using a bright field microscope (Nikon Eclipse E800), the number of beads was counted using a segmentation algorithm in a Matlab program. To reuse the microfluidic control system, the solid substrate is peeled away from the fluidic layers, and the fluidic device is rinsed with IPA and DI water sequentially. For the next assay, a new solid substrate is bonded as described above.

Results and Discussion

Lifting gate microvalves and pumps were developed and characterized for break-through pressure and pumping efficiency. Figure 3 presents a characterization of the fluid flow through a lifting gate microvalve. The closing pressure required to hold off an applied fluidic pressure increases linearly with the applied pressure. The maximum break-through pressure observed was 65 kPa with a 50 kPa closing pressure.

Pumping rates (nL/s) as a function of closing pressure and actuation time were measured gravimetrically (see supporting information). The actuation time is the length of time each valve remains opened or closed for a given step of the program. The volume pumped per cycle was then calculated using the measured pumping rate. Figure 4A shows volume pumped per cycle as a function of actuation time and closing pressure for the pump containing a 3.75 mm diameter diaphragm valve (pump 5 in Figure 1B). At fixed actuation times, the volume pumped per cycle increases with increasing closing pressure. It can be

inferred that low closing pressure results in some backflow in the pump while high closing pressure increases the efficiency of fluid transfer between valves. When the closing pressure approached 45 kPa and the actuation time exceeded 600 ms, the volume pumped per cycle reaches a maximum level of 680 ± 2.4 nL ($86.2 \pm 0.72\% V_{\max}$). This maximum efficiency is slightly higher than that previously reported for monolithic membrane valves ($82\% V_{\max}$).¹⁹ At fixed closing pressures greater than 10 kPa, the volume pumped per cycle increased with increasing actuation time and approached the maximum efficiency since sufficient actuation time is required for complete filling or emptying of the diaphragm valve. As the closing pressure increased, the actuation time required for maximum efficiency decreased as expected. In addition, the diameter of the diaphragm valve was found to affect the pumping efficiency in terms of volume pumped per cycle. As the diameter of diaphragm valve decreases, the actuation time required for maximum efficiency decreases (Figure S-2). Smaller sized microvalves have sufficient time to transfer the liquid while closing the gate structure under lower closing pressure. As expected, a longer actuation time is necessary to achieve maximum efficiency for larger microvalves at low closing pressure.

The maximum volume pumped per cycle was determined for each pump by varying the actuation time at 30 kPa closing pressure. The maximum volume pumped per cycle increases linearly with the volume of the diaphragm displacement chamber. Regardless of diaphragm valve size, the maximum volume pumped per cycle was found to be $86.2\% V_{\max}$ (Figure 4B). Using this relationship, we can design the required chamber size for precise metering of nanoliter scale volumes.

To demonstrate the utility of the lifting gate microvalves and pumps, we fabricated a programmable sample processing system with an integrated bioreactor for solid phase capture immunoassays (Figure 5). In this example, the lifting gate microvalves were used to automate each of the steps in a microparticle label immunoassay for mouse IgG detection. Using streptavidin functionalized PET as a solid support, biotinylated anti-mouse Ig-F_C, 1% BSA, mouse IgG and anti-mouse IgG conjugated microparticle were pumped sequentially through reaction chamber. Washing of unbound microparticles was performed hydrodynamically by pumping buffer through the reaction chamber. Figure 5B shows the results of the 15 minute assay for a negative and 1 $\mu\text{g/mL}$ mouse IgG target concentration using a single device. Using this device, a signal to noise of 7.39 ± 0.37 was achieved. These results indicated that the lifting gate microvalves are useful for automated immunoassay applications with significantly reduced fabrication complexity. The increase in bead density for the positive sample can also be observed with the naked eye, enabling rapid and portable biomarker analysis. Since lifting gate microvalves can be directly bonded to a variety of substrates, they can be used as a control system for other microdevices using this modular assembly. We previously demonstrated an automated, microfluidic microparticle labeled immunoassay platform using normally closed monolithic membrane valves.¹⁰ This microfluidic platform required additional layers for integration and more complex fabrication processes such as glass etching, thin PDMS film formation, and drilling via-holes in glass. The lifting gate microfluidic control system has significantly reduced fabrication complexity, facile integration with plastic substrates, and high-performance bioassay capabilities.

We have demonstrated that pneumatically actuated lifting gate microvalves and pumps can be directly integrated with a wide range of substrates. The use of closing pressures in the range of 30-45 kPa significantly reduces the hysteresis previously reported for similar microvalves²⁶ and enables high-efficiency, integrated pumping operations. These structures also enable separate fabrication of the microfluidic platform and functional surface, thereby simplifying the process for device fabrication and assembly. The modular design and assembly of such systems provides an appropriate format for a disposable microfluidic

sample processing system and/or a point-of-care diagnostic device. Furthermore, by adjusting the height of the lifting gate, we can fabricate both normally-closed and normally-open microvalves. This ability is especially useful for the filtration of particles such as cells by precisely controlling the actuation pressure.

Supplementary Material

Refer to Web version on PubMed Central for supplementary material.

Acknowledgments

Financial support for this work was provided by grant U54ES016115 from the U.S. National Institute for Environmental Health Sciences (NIEHS) through the trans-NIH Genes, Environment and Health Initiative. The devices were fabricated in the UC Berkeley Micro-lab and Bio-Nanotechnology Center (BNC).

References

1. Blazej RG, Kumaresan P, Mathies RA. *Proc Natl Acad Sci U S A*. 2006; 103:7240–7245. [PubMed: 16648246]
2. Easley CJ, Karlinsky JM, Bienvenue JM, Legendre LA, Roper MG, Feldman SH, Hughes MA, Hewlett EL, Merkel TJ, Ferrance JP, Landers JP. *Proc Natl Acad Sci U S A*. 2006; 103:19272–19277. [PubMed: 17159153]
3. Fan HC, Wang J, Potanina A, Quake SR. *Nat Biotechnol*. 2011; 29:51–57. [PubMed: 21170043]
4. Liu P, Mathies RA. *Trends Biotechnol*. 2009; 27:572–581. [PubMed: 19709772]
5. Beyor N, Seo T, Liu P, Mathies R. *Biomed Microdev*. 2008; 10:909–917.
6. Wang CH, Lee GB. *Biosens Bioelectron*. 2005; 21:419–425. [PubMed: 16076430]
7. Zaytseva NV, Goral VN, Montagna RA, Baeumner AJ. *Lab Chip*. 2005; 5:805–811. [PubMed: 16027930]
8. Jensen EC, Zeng Y, Kim J, Mathies RA. *JALA*. 2010; 15:455–463. [PubMed: 21218162]
9. Gao X, Jiang L, Su X, Qin J, Lin B. *Electrophoresis*. 2009; 30:2481–2487. [PubMed: 19639569]
10. Kim J, Jensen E, Megens M, Boser B, Mathies RA. *Lab Chip*. 2011; 11:3106–3112. [PubMed: 21804972]
11. Zeng Y, Novak R, Shuga J, Smith MT, Mathies RA. *Anal Chem*. 2010; 82:3183–3190. [PubMed: 20192178]
12. Zare RN, Kim S. *Annu Rev Biomed Eng*. 2010; 12:187–201. [PubMed: 20433347]
13. Mary P, Chen A, Chen I, Abate AR, Weitz DA. *Lab Chip*. 2011; 11:2066–2070. [PubMed: 21541376]
14. Novak R, Zeng Y, Shuga J, Venugopalan G, Fletcher DA, Smith MT, Mathies RA. *Angew Chem Int Ed*. 2011; 50:390–395.
15. Jensen EC, Bhat BP, Mathies RA. *Lab Chip*. 2010; 10:685–691. [PubMed: 20221555]
16. Oh KW, Ahn CH. *J Micromech Microeng*. 2006; 16:R13–R39.
17. Thorsen T, Maerkl SJ, Quake SR. *Science*. 2002; 298:580–584. [PubMed: 12351675]
18. Unger MA, Chou HP, Thorsen T, Scherer A, Quake SR. *Science*. 2000; 288:113–116. [PubMed: 10753110]
19. Grover WH, Skelley AM, Liu CN, Lagally ET, Mathies RA. *Sens Act B*. 2003; 89:315–323.
20. Grover WH, Ivester RH, Jensen EC, Mathies RA. *Lab Chip*. 2006; 6:623–631. [PubMed: 16652177]
21. Zhang W, Lin S, Wang C, Hu J, Li C, Zhuang Z, Zhou Y, Mathies RA, Yang CJ. *Lab Chip*. 2009; 9:3088–3094. [PubMed: 19823724]
22. Skelley AM, Scherer JR, Aubrey AD, Grover WH, Ivester RHC, Ehrenfreund P, Grunthaner FJ, Bada JL, Mathies RA. *Proc Natl Acad Sci U S A*. 2005; 102:1041–1046. [PubMed: 15657130]
23. Holden MA, Jung SY, Cremer PS. *Anal Chem*. 2004; 76:1838–1843. [PubMed: 15053641]

24. Schudel BR, Choi CJ, Cunningham BT, Kenis PJ. *Lab Chip*. 2009; 9:1676–1680. [PubMed: 19495449]
25. Bhattacharyya A, Klapperich CM. *Lab Chip*. 2007; 7:876–882. [PubMed: 17594007]
26. Mohan R, Schudel BR, Desai AV, Yearsley JD, Apblett CA, Kenis PJA. *Sens Act B*. 2011; 160:1216–1223.

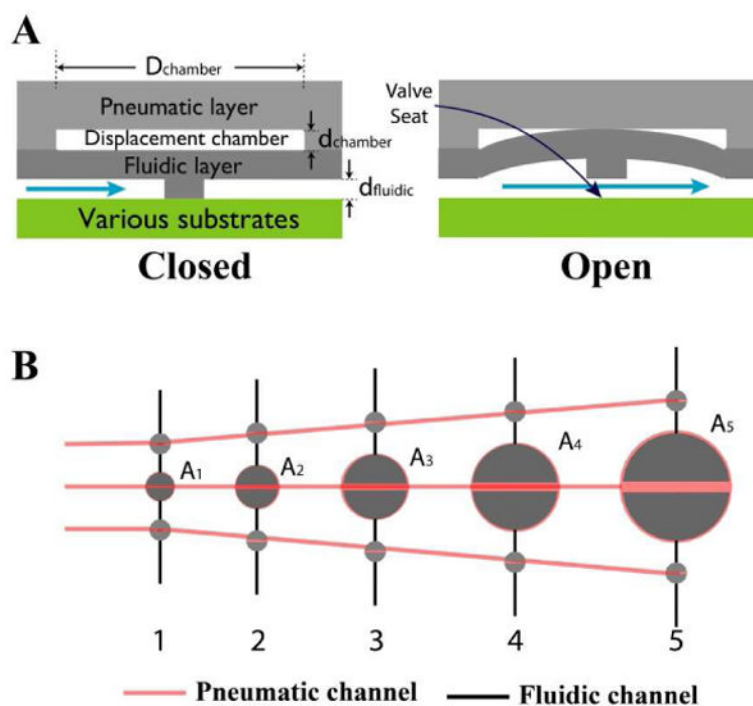


Figure 1.

(A) Cross-sectional view of normally closed PDMS “lifting gate” microvalve. Displacement chambers formed in a PDMS pneumatic layer are aligned and permanently bonded with a PDMS fluidic layer containing gate structures. The opposite side of the fluidic layer can be bonded to a variety of substrates to form hybrid channels. Application of a vacuum to the displacement chamber pulls the gate structure away from the substrate, filling and allowing fluid flow through the microvalve. (B) Layout of micropumps formed from three PDMS gate lifting microvalves in series used for testing. A_i ($i= 1\sim 5$) presents a half of fluidic chamber area.

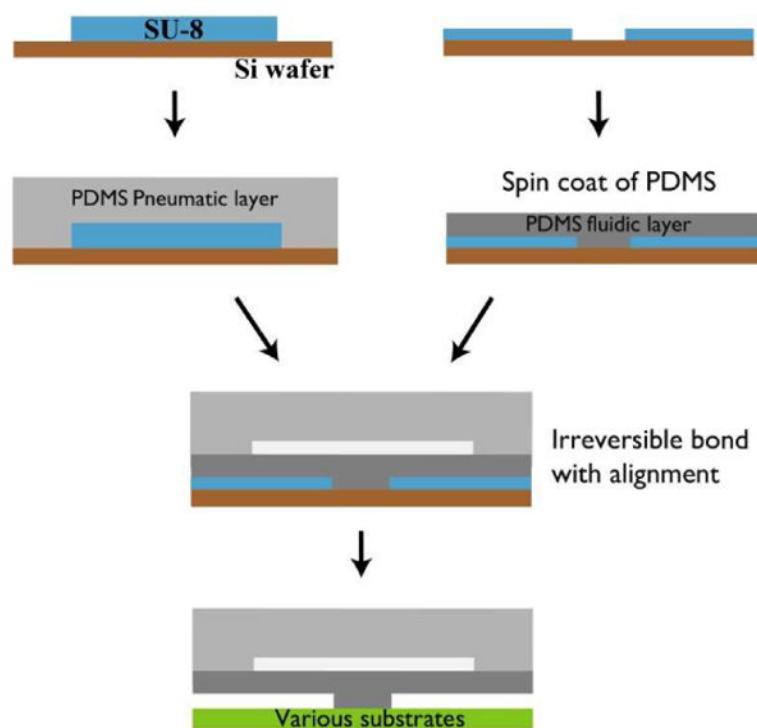


Figure 2. Illustration of fabrication process for PDMS lifting gate microvalves. The fluidic and pneumatic layers are created using a soft-lithography method. For the pneumatic layer, uncured PDMS is poured onto a SU8 mold to create a ~ 4 mm thick layer. For the channel layer, uncured PDMS was spun onto a mold at 350 rpm to achieve ~ 200 μm thick films with the channel structures. The two layers are bonded together after oxygen plasma treatment and then attached to a selected substrate.

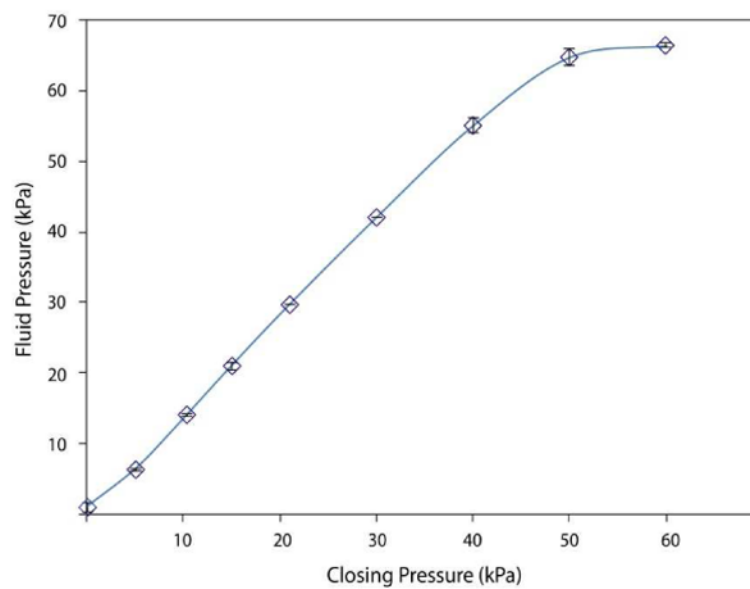


Figure 3. Fluid pressure required to initiate flow through a valve being held at the indicated manifold (closing) pressure with a 2.25 mm diameter microvalve (N=4).

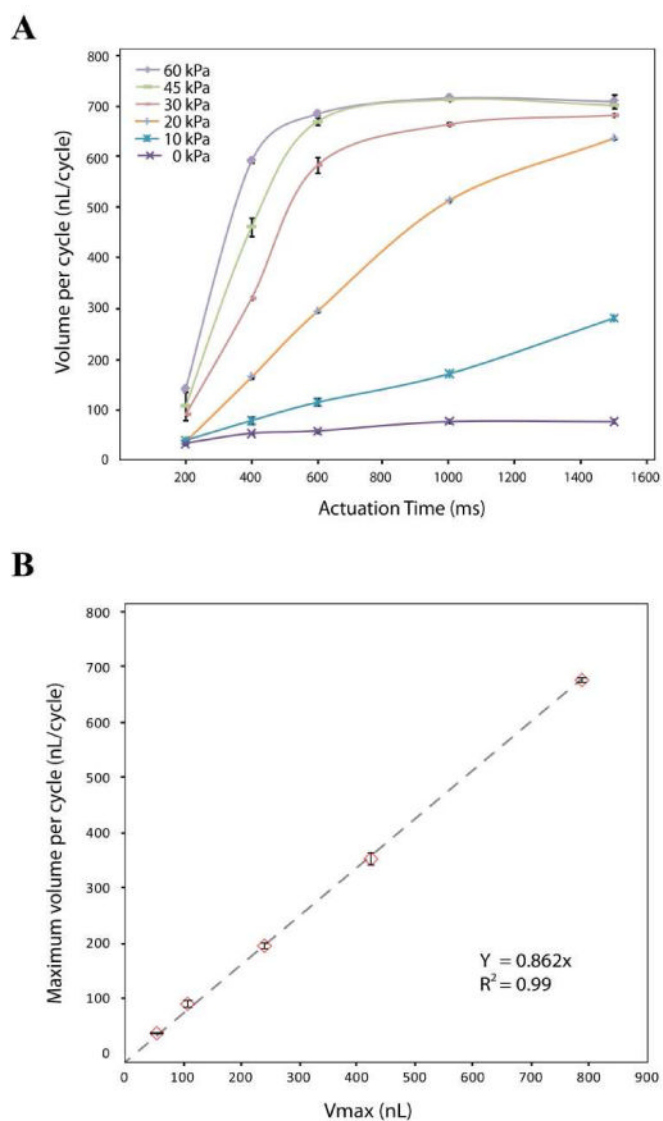


Figure 4. (A) Volume pumped per cycle as a function of actuation time and closing pressure for pump 5 (3.75mm diameter) in Figure 1B. Valve actuation vacuum was -87 kPa and pressure was varied from 0 to 60 kPa. (B) Maximum volume pumped per cycle as a function of diaphragm chamber volume for pumps 1 through 5 shown in Figure 1A. Valve actuation and pressure were -87 and 30 kPa, respectively.

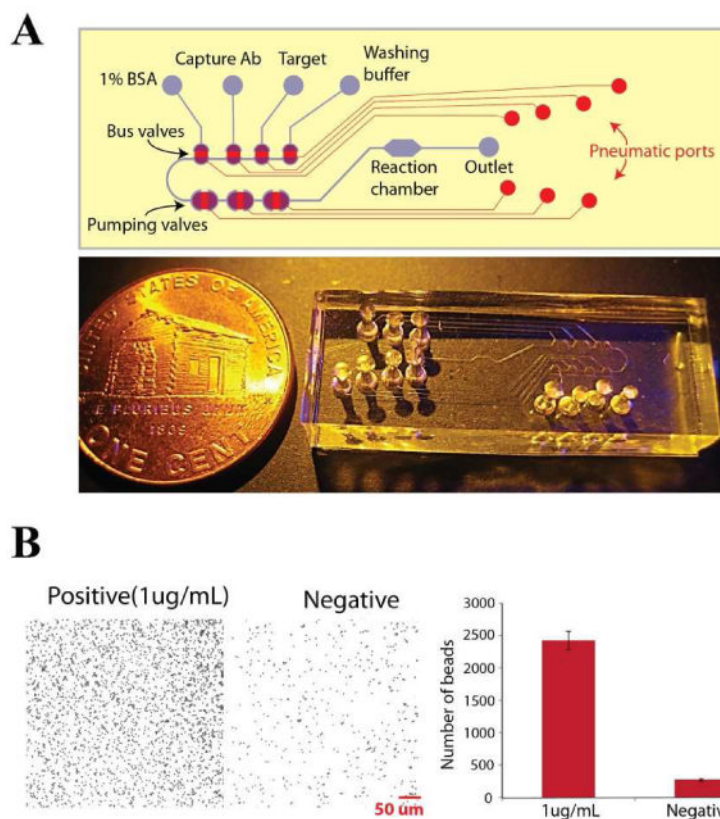


Figure 5. (A) Automated microparticle based immunoassay with lifting gate microvalves and pumps. After UV ozone treatment of the PDMS layer, it was manually bonded to a polyester terephthalate (PET) substrate treated with streptavidin. Four bus valves were used for selecting buffer and reagents while flow through the reactor was controlled by the pumping valves. (B) Results of the automated microparticle label immunoassay for 1 $\mu\text{g}/\text{mL}$ mouse IgG and blank samples. The number of beads specifically bound to surfaces was counted from optical micrographs (N=3).